



Synthesis, structures and magnetic properties of copper(II) complexes with 1,2,3-triazole derivate as ligand: a single-crystal-to-single-crystal transformation from mononuclear to polymeric complex of copper(II)

Fan Ouyang¹ · Xiaofeng Jiang¹ · Xianlong Liu¹ · Yunzhou Chen¹ · Yunfeng Chen¹ · Sihuai Chen¹ · Lihui Jia^{1,2}

Received: 25 September 2020 / Accepted: 7 January 2021 / Published online: 23 January 2021
© The Author(s), under exclusive licence to Springer Nature Switzerland AG part of Springer Nature 2021

Abstract

A new mononuclear complex $\text{Cu}(\text{tdp})\text{Br}_2 \cdot \text{MeCN}$ (**1**, $\text{tdp} = 2,2'-(1\text{H}-1,2,3\text{-triazole-1,4-diyl})\text{dipyridine}$) has been synthesized, which can transform to a 1D coordination polymer $[\text{Cu}(\text{tdp})\text{Br}_2]_n$ (**2**) under ambient conditions through an irreversible single-crystal-to-single-crystal transformation process. The loss of lattice MeCN molecules in **1** was accompanied by the generation of new covalent bonds and an increase in dimensionality from 0 to 1D, leading to a change in magnetic exchange couplings between the adjacent Cu(II) ions. Magnetic susceptibility measurements indicate that **1** exhibits ferromagnetic interactions between the adjacent Cu(II) centers, while the intrachain magnetic interactions between Cu(II) ions are antiferromagnetic within **2**.

Introduction

The phenomenon of single-crystal-to-single-crystal (SCSC) transformation has attracted intense interest, since the structural transformation can be accompanied by changes in spectral [1–5] and magnetic properties [6–9], which offers promising perspectives toward developing innovative materials. For magnetic materials, SCSC transformations involving the breaking and formation of the coordination bonds may lead to the modification of metal–ligand environment and/or spin topology, and thus providing an effective strategy to

tune the magnetism and investigate the magneto-structural correlations [10–13].

So far, SCSC transformations have been widely used as a method for subtle modification in the coordination environment of metal ions and superexchange pathway in porous magnets, and most of which are induced by sorption/desorption of guest molecules, especially solvents [14–17]. However, due to the absence of voids for the guest molecules, only limited SCSC transformations generating a tunable magnetic system have been obtained in nonporous coordination polymers [18–22]. Furthermore, since the movement of molecules in the crystal form is restricted, SCSC transformation in the solid state is difficult [23–25].

One of the fruitful routes for achieving SCSC transformation is to design ligands with many potential donor atoms, which can provide various coordination modes. Pyridyl substituted triazoles contain two or more potentially conjugated aromatic rings with several N-donor coordination sites, possessing both chelating and bridging capabilities [26–29]. In particular, 1,2,4-triazole and its derivatives have been widely used for the construction of functional coordination complexes [30, 31], some of which implemented SCSC transformations [32, 33]. However, in comparison to 1,2,4-triazole derivatives, 1,2,3-triazole derivatives have been less studied in the synthetic chemistry of transition metal complexes due to their difficulties in synthesis [34–37]. In this work, we synthesized a new discrete nonporous mononuclear complex $\text{Cu}(\text{tdp})\text{Br}_2 \cdot \text{MeCN}$ (**1**, $\text{tdp} = 2,2'-(1\text{H}-1,2,3\text{-triazole-1,4-diyl})$

Supplementary information The online version of this article (<https://doi.org/10.1007/s11243-021-00448-6>) contains supplementary material, which is available to authorized users.

✉ Sihuai Chen
sihuai_chen@wit.edu.cn

✉ Lihui Jia
jjalihui715@wit.edu.cn

¹ Key Laboratory for Green Chemistry Process of Ministry of Education, School of Chemistry and Environmental Engineering, Wuhan Institute of Technology, Wuhan 430073, People's Republic of China

² Ministry-of-Education Key Laboratory for the Synthesis and Application of Organic Function Molecules, College of Chemistry and Chemical Engineering, Hubei University, Wuhan 430062, People's Republic of China

dipyridine). Compound **1** transformed to a 1D chain $[\text{Cu}(\text{tdp})\text{Br}_2]_n$ (**2**) under ambient conditions through an irreversible liquid free SCSC transformation process. To the best of our knowledge, the coordination chemistry of this ligand has still rarely been reported [38–41]. Herein, we described the synthesis, structures and magnetic properties of both compounds.

Experimental

Materials and general methods

All materials used in the experiment were commercially available at analytical grade and used without further purification. Elemental analysis of C, H, N was performed using an Elementar Vario EL analyzer. The FT-IR spectra were recorded from KBr pellets in the range $4000\text{--}400\text{ cm}^{-1}$ on a Bruker Tensor II Spectrum FT-IR spectrometer. PXRD data were collected in the range of $5\text{--}50^\circ$ for 2θ on crystalline samples using a Rigaku Dmax 2000 diffractometer with $\text{Cu K}\alpha$ radiation ($\lambda = 0.15418\text{ nm}$, 40 kV, 40 mA) in flat-plate geometry at room temperature.

Synthesis of 2,2'-(1H-1,2,3-triazole-1,4-diyl)dipyridine (*tdp*)

The ligand 2,2'-(1H-1,2,3-triazole-1,4-diyl)dipyridine (*tdp*) was prepared according to the literature in 2 steps [42].

Synthesis of 4-pyridyl-NH-1,2,3-triazole

The mixture of pyridine-2-carboxaldehyde (2.14 g, 20.00 mmol), nitromethane (1.83 g, 30.00 mmol), NaN_3 (1.56 g, 24.00 mmol) and AlCl_3 (0.27 g, 2.00 mmol) was stirred in 40 mL DMSO at 70°C under air. After 5–8 h (as monitored by TLC), the solution was extracted with EtOAc ($3 \times 40\text{ mL}$). The combined organic layers were dried over anhydrous Na_2SO_4 , and the solvent was evaporated in vacuo. The resulting mixture was chromatographed on silica gel by eluting with ethyl acetate/petroleum ether (v/v 1:3) to afford 4-pyridyl-NH-1,2,3-triazole as yellow solids. Yield: 1.55 g (52.9%).

Synthesis of *tdp*

The mixture of 4-pyridyl-NH-1,2,3-triazole (0.50 g, 3.42 mmol), anhydrous K_2CO_3 (0.95 g, 6.84 mmol), L-proline (0.08 g, 0.68 mmol), 2-bromopyridine (0.65 g, 4.11 mmol) and CuCl (0.034 g, 0.34 mmol) was stirred in 25 mL DMSO at 100°C under anhydrous and anaerobic conditions. After 12 h (as monitored by TLC), the solution was extracted with EtOAc ($3 \times 40\text{ mL}$). The combined

organic layers were dried over anhydrous Na_2SO_4 , and the solvent was evaporated in vacuo. The resulting mixture was chromatographed on silica gel by eluting with ethyl acetate/petroleum ether (v/v 1:10) to afford *tdp* as white powders. Yield: 0.14 g (20.1%). IR (KBr): 3172(w), 3056(w), 1589(m), 1466(s), 1425 (m), 1233(m), 1018(s), 782(s), 731(m), 506(w).

Synthesis of $\text{Cu}(\text{tdp})\text{Br}_2 \cdot \text{MeCN}$ (**1**)

$\text{CuBr}_2 \cdot 2\text{H}_2\text{O}$ (0.066 mmol, 14.7 mg) was dissolved in 3 mL MeCN and added to a solution of *tdp* (0.066 mmol, 14.7 mg) in MeCN (6 mL), then the mixture was placed at room temperature. Brown crystals precipitated after a few minutes. Yield based on $\text{CuBr}_2 \cdot 2\text{H}_2\text{O}$: 70%. Elem. Anal. Calc. for $\text{C}_{14}\text{H}_{12}\text{Br}_2\text{CuN}_6$: C 34.48; H 2.48; N 17.23%; found: C 34.11; H 2.23; N 17.56%. Selected IR bands (KBr): 3098(m), 1594(m), 1577(m), 1454(s), 1283(m), 1251(w), 1211(w), 1065(m), 990(w), 785(s), 738(w), 502(w).

Synthesis of $[\text{Cu}(\text{tdp})\text{Br}_2]_n$ (**2**)

There are 2 methods to obtain **2**. Method A: placing **1** in the air for 10 days, the brown crystals transformed to green blocks slowly. Method B: placing **1** (5 mg) in MeCN (5 mL), the mixture was then heated at 90°C for 3 days in a furnace and naturally cooled to room temperature to obtain the green block crystals. Elem. Anal. Calc. for $\text{C}_{12}\text{H}_9\text{Br}_2\text{CuN}_5$: C 32.27; H 2.03; N 15.68%; found: C 32.43; H 2.20; N 15.69%. Selected IR bands (KBr): 3098(s), 3058(w), 1594(m), 1456(s), 1287(m), 1254(w), 1148(w), 1066(m), 1021(w), 991(w), 787(s), 740(w), 503(w).

X-ray crystallography

The X-ray crystallographic data for the single crystals of both compounds were collected on an XtaLAB Mini (Rigaku OD, 2015) employing graphite-monochromated $\text{Mo K}\alpha$ radiation ($\lambda = 0.71073\text{ \AA}$) at 293 K. An empirical absorption correction was applied using spherical harmonics implemented in SCALE3 ABSPACK scaling algorithm. Complexes **1** and **2** were solved by intrinsic phasing using the Olex2 program with the SHELXS package and refined with SHELXL [43–45]. All the non-hydrogen atoms were refined anisotropically. Hydrogen atoms were placed in calculated positions, refined using idealized geometries (riding model) and assigned fixed isotropic displacement parameters. For compound **2**, the disorder in *tdp* ligand was modeled using sets of isotropic atoms of 50% occupancy. Details of the crystal, data collection and refinement parameters are listed in Table S1, and selected bond lengths and bond angles are given in Table S2.

Magnetic measurements

Magnetic measurements for **1** and **2** were performed on a MPMS XL-5 SQUID (Superconducting Quantum Interference Device) on finely ground polycrystalline samples. The dc magnetic susceptibility data were collected in the 2.0–300 K temperature range at 1000 Oe. Low-temperature isothermal magnetization was measured with an applied field from 0 till 5 T. All data were corrected for the contribution of the sample holder and for the diamagnetism estimated from Pascal's constants [46].

Results and discussion

Synthesis and crystal structures

The reaction of CuBr_2 and *tdp* ligand in the molar ratio 1:1 in MeCN at room temperature afforded the mononuclear compound $\text{Cu}(\text{tdp})\text{Br}_2 \cdot \text{MeCN}$ (**1**). The 1D coordination polymer $[\text{Cu}(\text{tdp})\text{Br}_2]_n$ (**2**) was synthesized *via* a structural transformation of **1** in a SCSC manner under ambient conditions. Single-crystal X-ray diffraction studies revealed that

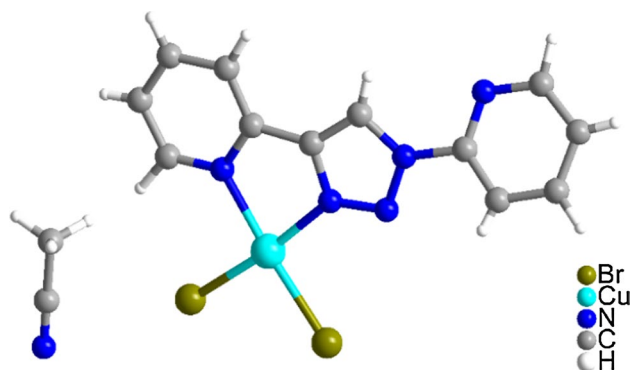
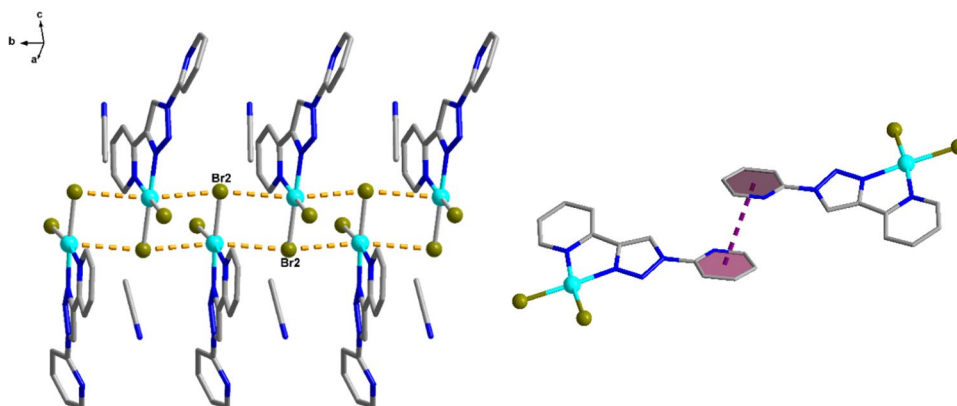


Fig. 1 Molecular structure of compound **1**

Fig. 2 One-dimensional Cu^{II} chains (left) and $\pi \cdots \pi$ interactions between aromatic rings of 2 adjacent chains (right) for compound **1**. Hydrogen atoms have been omitted for clarity

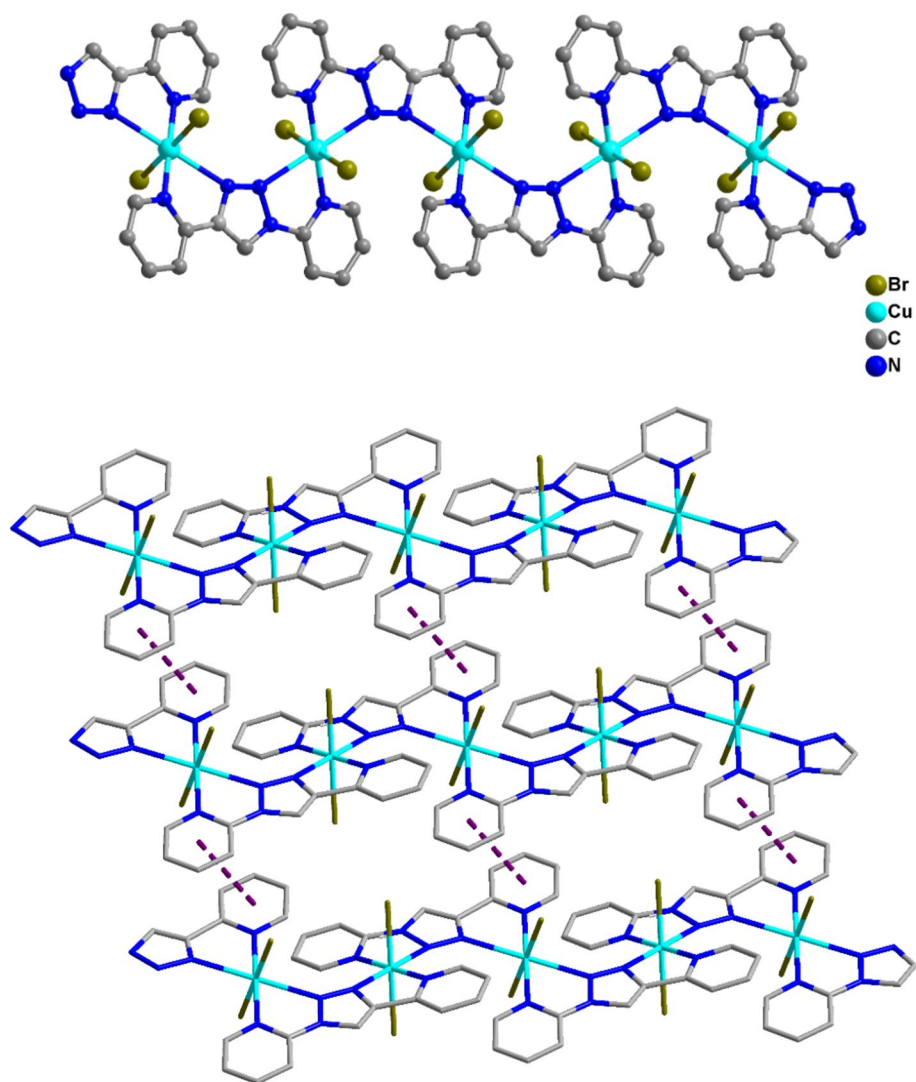


both compounds **1** and **2** crystallize in the monoclinic space group $C2/c$.

As shown in Fig. 1, compound **1** has one lattice MeCN per molecule. The molecular structure of **1** consists of a tetracoordinate Cu^{II} with a square planar geometry through 2 nitrogen atoms from the chelating *tdp* ligand and 2 bromine atoms. The average Cu–N and Cu–Br bond lengths are all in the normal ranges (Table S2). The coordination geometry of Cu^{II} centers was analyzed with SHAPE 2.0 software, showing a continuous shape measurement (*CShM*) of 1.13, confirming the distorted square planar coordination of Cu^{II} ions. The Br2 atoms from both neighboring molecules in the axial directions are located at distances of 3.243 and 3.294 Å, respectively. The adjacent molecular units are further connected via 2 axial $\text{Cu} \cdots \text{Br}_2$ supramolecular interactions to form a one-dimensional chain (Fig. 2, left). The $\text{Cu} \cdots \text{Cu}$ distance is 3.95 Å. Furthermore, there are weak $\pi \cdots \pi$ interactions between aromatic ring planes of two adjacent chains within **1**, leading to the stabilization of the molecular packing. The centroid-to-centroid distances between the two nearest parallel aromatic ring planes are 3.758 Å (Fig. 2, right).

Compound **2** is a neutral 1D coordination polymer (Fig. 3, top). The Cu^{II} ions are six-coordinate, exhibiting a distorted octahedral coordination geometry with a continuous shape measurement (*CShM*) of 2.16. Both axial positions of the Cu^{II} ions are occupied by the nitrogen atoms of the triazole rings, while the equatorial plane is coordinate by 2 bromides and 2 pyridyl nitrogen atoms. Due to the Jahn–Teller effect, the axial Cu–N distances of 2.442 Å are rather longer than the equatorial Cu–N distances of 1.995 Å, while the equatorial Cu–Br distances are 2.491 Å in the normal range. The *tdp* ligands bridge the neighboring Cu^{II} ions in a bis-bidentate chelating mode and the intrachain $\text{Cu} \cdots \text{Cu}$ distances are 5.412 Å. Furthermore, the molecular packing of **2** is also stabilized by the $\pi \cdots \pi$ interactions between pyridine rings of 2 adjacent chains, and the centroid-to-centroid distance is 3.841 Å (Fig. 3, bottom).

Fig. 3 Linear structure of compound **2** (top) and $\pi\cdots\pi$ interactions between pyridine rings of 2 adjacent chains (bottom). Hydrogen atoms have been omitted for clarity



SCSC transformation

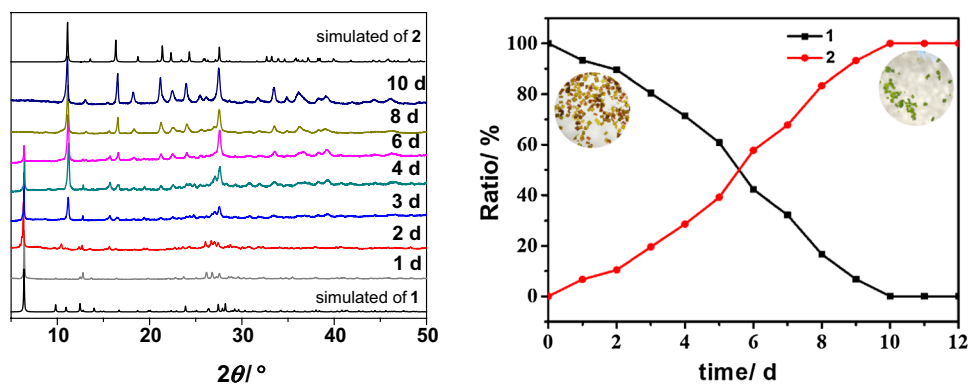
The brown single crystals of monomer **1** transformed to green single crystals of 1D chain $[\text{Cu}(\text{tdp})\text{Br}_2]_n$ (**2**) by separating them from the mother liquor and then leaving the crystals in the air for ten days. On the other hand, a transformation from **2** to **1** cannot be obtained, suggesting that **2** is the thermodynamically favored compound, while **1** represents the metastable compound. Furthermore, compound **2** can be synthesized by placing a small amount of **1** in 5 ml MeCN in an oven at 90 °C for 72 h under solvothermal conditions, confirming that **2** is thermodynamically favored. The SCSC transformation from **1** to **2** was further confirmed by powder X-ray diffraction (PXRD) patterns and the percentage conversion versus time plot (Fig. 4). The PXRD patterns for different times show that the distinct peak at $2\theta = 6.4^\circ$ of compound **1** vanished gradually, whereas new peaks generated at $2\theta = 11.1, 16.5, 21.1, 24.0$ and 27.5° slowly for compound **2**. After **1** was

placed in ambient air for 10 days, a sample with the same PXRD pattern of **2** was achieved.

However, if the crystals of **1** were placed under dry N_2 in a glass desiccator with a stopcock for ten days and PXRD data have been collected periodically (Fig. S1), the distinct peak at $2\theta = 6.4^\circ$ of **1** vanished gradually, whereas a new peak was generated at $2\theta = 7.6^\circ$ slowly, which was totally different from those for compound **2**. However, there were too many cracks in the obtained crystals, and their qualities were not good enough for SXRD analysis (Fig. S2). The structural transformation process under an inert atmosphere demands a single-crystal study of these obtained crystals, which will be the subject of our future work.

The difference between these processes suggested that some liquid phase (either air, moisture or MeCN in the case of solvothermal synthesis) should be present in order to achieve the structural transformation from **1** to **2**. By comparison with the crystal packing in **1** (Fig. S3) with the linear structure of **2** (Fig. 3), the structural transformation is likely

Fig. 4 PXRD patterns of **1** irradiated for different times (left) and plot of compound **1** and **2** obtained versus time (right)



to be associated with the rearrangement of molecules of **1** inside the layers, perpendicular to the *c*-axis. Both uncoordinated nitrogen atoms from the *tdp* ligands in **1** chelate the tetracoordinate Cu^{II} ions from the neighboring molecules, leading to an increase in coordination number of Cu^{II} from 4 to 6 and an increase in dimensionality from 0 to 1D.

Magnetic properties

Magnetic susceptibility for both compounds was collected on powdered samples in the 2.0–300 K temperature range (Fig. 5). The χT value at 300 K is 0.361 (for **1**) and 0.377 (for **2**) cm³ K mol⁻¹, respectively, which are all close to the expected value of 0.375 cm³ K mol⁻¹ for an isolated Cu^{II} ion ($S = 1/2$). The χT product for **1** increases with decreasing temperature, reaching a maximum value of 0.414 cm³ K mol⁻¹ at about 40 K, followed by a sharp drop down to 0.307 cm³ K mol⁻¹ at 2.0 K. This behavior indicates the presence of dominant ferromagnetic interactions between neighboring spin carriers, and the final decrease in χT might be due to the interchain antiferromagnetic interactions, which is likely to be attributed to the $\pi \cdots \pi$ stacking between the aromatic rings from the adjacent ligands. For **2**, the χT product almost keeps constant with decreasing temperature until it reaches 10 K, and then drops to 0.270 cm³ K mol⁻¹

at 2.0 K, suggesting the presence of dominant antiferromagnetic interactions within compound **2**.

The experimental data for both compounds have been further analyzed using the Baker's equation for a 1D Heisenberg chain of $S = 1/2$ system based on the spin Hamiltonian given below [47].

$$\hat{H} = -J\hat{S}_i\hat{S}_i \quad (1)$$

Thus, the magnetic susceptibility data were fitted to the following equation

$$\chi = \frac{Ng^2\beta^2}{4k_B T} \left(\frac{A}{B}\right)^{2/3} \quad (2)$$

where $A = 1.0 + 5.7979916y + 16.902653y^2 + 29.376885y^3 + 29.832959y^4 + 14.036918y^5$, $B = 1.0 + 2.7979916y + 7.0086780y^2 + 8.563644y^3 + 4.5743114y^4$ and $y = J/2k_B T$, and the interchain interactions zJ' have been taken into account as a mean-field correction

$$\chi_{\text{chain}} = \frac{\chi}{1 - \chi(2zJ'/Ng^2\beta^2)} \quad (3)$$

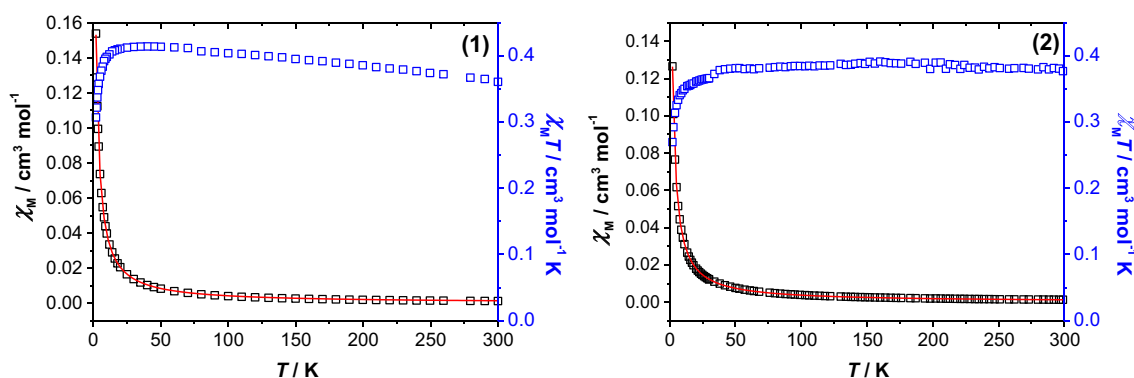


Fig. 5 Temperature dependence of χ and χT product for **1** and **2**. The solid line is the best-fit of the experimental data to the theoretical model

Table 1 The best-fit values of the magnetic susceptibility data to Eq. 3

	<i>g</i>	<i>J</i> (cm ⁻¹)	<i>J'</i> (cm ⁻¹)	<i>R</i>
1	2.13	0.23	-0.40	6.70 × 10 ⁻⁸
2	2.01	-1.81	-0.22	1.10 × 10 ⁻⁸

where $z = 2$. The best-fit values of the experimental data are summarized in Table 1, and R is defined as $R = \sum (\chi_M^{\text{calcd}} - \chi_M^{\text{obs}})^2 / \sum (\chi_M^{\text{obs}})^2$.

The best-fit values for **1** are close to those obtained in the reported mononuclear quasi-square Cu^{II}(Hmbm)Cl₂ monomers [48], confirming that the magnetic exchange interactions between the adjacent Cu^{II} ions for compound **1** are ferromagnetic, while the interactions through $\pi \cdots \pi$ stacking between the aromatic rings from the adjacent ligands are antiferromagnetic. However, the intra- and interchain interactions within **2** are both antiferromagnetic. According to the calculation [49], the antiferromagnetic component of J reaches its maximum for the parameters M–N–N = 135° and N–M–N = 90°. In our case, the Cu–N–N (144.5°) and N–Cu–N (74.2°) angles deviated from 135° and 90° resulting in weaker antiferromagnetic interactions. Thus, the observation of weak intrachain antiferromagnetic interaction within **2** is also reasonable.

Conclusion

In conclusion, a new mononuclear complex Cu(*tdp*)Br₂·MeCN (**1**) has been synthesized, which can transform to a 1D coordination polymer [Cu(*tdp*)Br₂]_n (**2**) under ambient conditions through an irreversible SCSC transformation process, accompanied by a change in magnetic properties. The dc magnetic susceptibility studies for both compounds revealed the presence of weak ferromagnetic interactions between the spin carriers within **1** and antiferromagnetic intrachain magnetic exchange couplings within **2**. Furthermore, the $\pi \cdots \pi$ stacking leads to the weak antiferromagnetic interactions within both compounds.

Supplementary material

Crystallographic data for the structural analysis have been deposited with the Cambridge Crystallographic Data Center. CCDC reference numbers are 2,020,059 (for **1**) and 2,020,060 (for **2**). Materials, reagent information, detailed synthetic procedures, instrument methods and crystallographic tables associated with this article can be found in

the online version. The crystallographic data can be found in the supporting information or can be obtained free of charge from the Cambridge Crystallographic Data Center via <https://summary.ccdc.cam.ac.uk/structure-summary-form>.

Acknowledgements We are grateful to the National Natural Science Foundation of China (21002076, 21441007), the Open Fund Project NO. KLSAOFM1709 of Ministry-of-Education Key Laboratory for the Synthesis and Application of Organic Function Molecules, Hubei University and the Science Foundation of Wuhan Institute of Technology (19QD37).

Compliance with ethical standards

Conflict of interest The authors declare that there are no conflicts of interest to this work.

References

- Song XZ, Song SY, Zhao SN, Hao ZM, Zhu M, Meng X, Wu LL, Zhang HJ (2014) Single-crystal-to-single-crystal transformation of a europium(III) metal-organic framework producing a multi-responsive luminescent sensor. *Adv Funct Mater* 24:4034–4041
- Jassal AK, Sharma S, Hundal G, Hundal MS (2015) Structural diversity, thermal studies, and luminescent properties of metal complexes of dinitrobenzoates: a single crystal to single crystal transformation from dimeric to polymeric complex of copper(II). *Cryst Growth Des* 15:79–93
- Jin M, Sumitani T, Sato H, Seki T, Ito H (2018) Mechanical-stimulation-triggered and solvent-vapor-induced reverse single-crystal-to-single-crystal phase transitions with alterations of the luminescence color. *J Am Chem Soc* 140:2875–2879
- Lee K, Lai PN, Parveen R, Donahue CM, Wymore MM, Massman BA, Vlasisavljevic B, Teets TS, Daly SR (2020) Modifying the luminescent properties of a Cu(I) diphosphine complex using ligand-centered reactions in single crystals. *Chem Commun*. <https://doi.org/10.1039/D0CC03427D>
- De Bellis J, Bellucci L, Bottaro G, Labella L, Marchetti F, Samaritano S, Dell'Amico DB, Armelao L (2020) Single-crystal-to-single-crystal post-synthetic modifications of three-dimensional LOFs (Ln=Gd, Eu): a way to modulate their luminescence and thermometric properties. *Dalton Trans* 49:6030–6042
- Kim Y, Das S, Bhattacharya S, Hong S, Kim MG, Yoon M, Natarajan S, Kim K (2012) Metal-ion metathesis in metal-organic frameworks: a synthetic route to new metal-organic Frameworks. *Chem-Eur J* 18:16642–16648
- Yang XF, Liu M, Zhu HB, Hang C, Zhao Y (2017) Syntheses, structures, and magnetic properties of two unique Cu(II)-based coordination polymers involving a crystal-to-crystal structural transformation from a 1D chain to a 3D network. *Dalton Trans* 46:17025–17031
- Chen WB, Chen YC, Huang GZ, Liu JL, Jia JH, Tong ML (2018) Cyclic off/part/on switching of single-molecule magnet behaviours via multistep single-crystal-to-single-crystal transformation between discrete Fe(II)–Dy(III) complexes. *Chem Commun* 54:10886–10889
- Clements JE, Airey PR, Ragon F, Shang V, Kepert CJ, Neville SM (2018) Guest-adaptable spin crossover properties in a dinuclear species underpinned by supramolecular interactions. *Inorg Chem* 57:14930–14938

- Sato O, Tao J, Zhang YZ (2007) Control of magnetic properties through external stimuli. *Angew Chem Int Ed* 46:2152–2187
- Wang LF, Qiu JZ, Liu JL, Chen YC, Jia JH, Jover J, Ruiz E, Tong ML (2015) Modulation of single-molecule magnet behaviour via photochemical [2 + 2] cycloaddition. *Chem Commun* 51:15358–15361
- Tian H, Su JB, Bao SS, Kurmoo M, Huang XD, Zhang YQ, Zheng LM (2018) Reversible ON–OFF switching of single-molecule-magnetism associated with single-crystal-to-single-crystal structural transformation of a decanuclear dysprosium phosphonate. *Chem Sci* 9:6424–6433
- Huang XD, Xu Y, Fan K, Bao SS, Kurmoo M, Zheng LM (2018) Reversible SC–SC transformation involving [4 + 4] cycloaddition of anthracene: a single-ion to single-molecule magnet and yellow-green to blue-white emission. *Angew Chem Int Ed* 57:8577–8581
- Moulton B, Zaworotko MJ (2001) From molecules to crystal engineering: supramolecular isomerism and polymorphism in network solids. *Chem Rev* 101:1629–1658
- Zhang JP, Liao PQ, Zhou HL, Lin RB, Chen XM (2014) Single-crystal X-ray diffraction studies on structural transformations of porous coordination polymers. *Chem Soc Rev* 43:5789–5814
- Meng Y, Dong YJ, Yan Z, Chen YC, Song XW, Li QW, Zhang CL, Ni ZP, Tong ML (2018) A new porous three-dimensional Iron(II) coordination polymer with solvent-induced reversible spin-crossover behavior. *Cryst Growth Des* 18:5214–5219
- Liu ZY, Zhao H, Song WC, Wang XG, Liu ZY, Zhao XJ, Yang EC (2019) A dynamic microporous magnet exhibiting room-temperature thermal hysteresis, variable magnetic ordering temperatures and highly selective adsorption for CO₂. *J Mater Chem C* 7:218–222
- Li B, Wei RJ, Tao J, Huang RB, Zheng LS, Zheng Z (2010) Solvent-induced transformation of single crystals of a spin-crossover (SCO) compound to single crystals with two distinct SCO centers. *J Am Chem Soc* 132:1558–1566
- Wei RJ, Tao J, Huang RB, Zheng LS (2011) Reversible and irreversible vapor-induced guest molecule exchange in spin-crossover compounds. *Inorg Chem* 50:8553–8564
- Chaudhary A, Mohammad A, Mobin SM (2017) Recent advances in single-crystal-to-single-crystal transformation at the discrete molecular level. *Cryst Growth Des* 17:2893–2910
- Chen WB, Chen YC, Yang M, Tong ML, Dong W (2018) Water molecule induced reversible single-crystal-to-single-crystal transformation between two trinuclear Fe(II) complexes with different spin crossover behaviour. *Dalton Trans* 47:4307–4314
- Tu J, Chen H, Tian H, Yu X, Zheng B, Zhang S, Ma P (2020) Temperature-induced structural transformations accompanied by changes in magnetic properties of two copper coordination polymers. *CrystEngComm* 22:3482–3488
- Kolea GK, Vittal JJ (2013) Solid-state reactivity and structural transformations involving coordination polymers. *Chem Soc Rev* 42:1755–1775
- He WW, Li SL, Lan YQ (2018) Liquid-free single-crystal to single-crystal transformations in coordination polymers. *Inorg Chem Front* 5:279–300
- Dmitrienko AO, Buzin MI, Setifi Z, Setifi F, Alexandrov EV, Voronova ED, Vologzhanina AV (2020) Solid-state 1D → 3D transformation of polynitrile-based coordination polymers by dehydration reaction. *Dalton Trans* 49:7084–7092
- Crowley JD, Bandeen PH, Hanton LR (2010) A one pot multi-component CuAAC “click” approach to bidentate and tridentate pyridyl-1,2,3-triazole ligands: synthesis, X-ray structures and copper(II) and silver(I) complexes. *Polyhedron* 29:70–83
- Prabhath MRR, Romanova J, Curry RJ, Silva SRP, Jarowski PD (2015) The role of substituent effects in tuning metallophilic interactions and emission energy of bis-4-(2-pyridyl)-1,2,3-triazoloplatinum(II) complexes. *Angew Chem Int Ed* 54:7949–7953
- Zhang Y, Chen Y, Zhou S, Meng X, Jia L, Chen Y (2017) Synthesis, structure and properties of a new NH-1,2,3-triazole-based octanuclear copper(II) complex. *Inorg Chem Commun* 84:159–163
- Conradie J, Conradie MM, Tawfiq KM, Coles SJ, Tizzard GJ, Wilson C, Potgieter JH (2018) Jahn–teller distortion in 2-pyridyl-(1,2,3)-triazole-containing copper(II) compounds. *New J Chem* 42:16335–16345
- Haasnoot JG (2000) Mononuclear, oligonuclear and polynuclear metal coordination compounds with 1,2,4-triazole derivatives as ligands. *Coord Chem Rev* 200–202:131–185
- Aromí G, Barrios LA, Roubeaub O, Gamez P (2011) Triazoles and tetrazoles: prime ligands to generate remarkable coordination materials. *Coord Chem Rev* 255:485–546
- Liu JY, Wang Q, Zhang LJ, Yuan B, Xu YY, Zhang X, Zhao CY, Wang D, Yuan Y, Wang Y, Ding B, Zhao XJ, Yue MM (2014) Anion-exchange and anthracene-encapsulation within copper(II) and manganese(II)-triazole metal–organic confined space in a single crystal-to-single crystal transformation fashion. *Inorg Chem* 53:5972–5985
- Wu XW, Pan F, Yin S, Ge JY, Jin GX, Wang P, Ma JP (2018) Solvent-induced structural transformation and magnetic modulation in 1D copper(II) polymers based on a semi-rigid ligand containing 4-amino-1,2,4-triazole. *CrystEngComm* 20:3955–3959
- Schweinfurth D, Sommer MG, Atanasov M, Demeshko S, Hohloch S, Meyer F, Neese F, Sarkar B (2015) The ligand field of the azido ligand: insights into bonding parameters and magnetic anisotropy in a Co(II)–Azido Complex. *J Am Chem Soc* 137:1993–2005
- Schweinfurth D, Hettmanczyk L, Suntrup L, Sarkar B (2017) Metal complexes of click-derived triazoles and mesoionic carbenes: electron transfer, photochemistry, magnetic bistability, and catalysis: metal complexes of click-derived triazoles and mesoionic carbenes: electron transfer, photochemistry, magnetic bistability, and catalysis. *Z Anorg Allg Chem* 643:554–584
- Chen Y, Chen XL, Chen Y, Jia L, Zeng MH (2017) Design, structure and magnetic properties of a novel one-dimensional Mn(II) coordination polymer constructed from 4-pyridyl-NH-1,2,3-triazole. *Inorg Chem Commun* 84:182–185
- Liu X, Chen M, Jiang X, Chen Y, Chen Y, Chen S, Jia L (2020) Two new 4-coordinate Cu(II) chains with 1,2,3-triazole derivate as bridging ligand: Synthesis, structures and magnetic properties. *J Mol Struct* 1217:128165
- McCarney EP, Hawes CS, Blasco S, Gunnlaugsson T (2016) Synthesis and structural studies of 1,4-di(2-pyridyl)-1,2,3-triazole dpt and its transition metal complexes; a versatile and subtly unsymmetric ligand. *Dalton Trans* 45:10209–10221
- Jindabot S, Teerachanan K, Thongkam P, Kiatisevi S, Khamnaen T, Phiriyawirut P, Charoenchaidet S, Sooksimuang T, Kongsaree P, Sangtrirutnugul P (2014) Palladium(II) complexes featuring bidentate pyridine–triazole ligands: synthesis, structures, and catalytic activities for Suzuki–Miyaura coupling reactions. *J Organomet Chem* 750:35–40
- Valencia M, Müller-Bunz H, Gossage RA, Albrecht M (2016) Enhanced product selectivity promoted by remote metal coordination in acceptor-free alcohol dehydrogenation catalysis. *Chem Commun* 52:3344–3347
- Thongkam P, Jindabot S, Prabpai S, Kongsaree P, Wititsuwannakul T, Surawatanawong P, Sangtrirutnugul P (2015) Pyridine–triazole ligands for copper-catalyzed aerobic alcohol oxidation. *RSC Adv* 5:55847–55855
- Hu Q, Liu Y, Deng X, Li Y, Chen Y (2016) Aluminium(III) chloride-catalyzed three-component condensation of aromatic aldehydes, nitroalkanes and sodium azide for the synthesis of 4-aryl-NH-1,2,3-TRIAZOLES. *Adv Synth Catal* 358:1689–1693

43. Sheldrick GM (2008) A short history of SHELX. *Acta Crystallogr Sect A* 64:112–122
44. Sheldrick GM (2015) Crystal structure refinement with SHELXL. *Acta Crystallogr Sect C* 71:3–8
45. Dolomanov OV, Bourhis LJ, Gildea RJ, Howad JAK, Puschmann M (2009) OLEX2: a complete structure solution, refinement and analysis program. *J Appl Cryst* 42:339–341
46. Kahn O (1993) *Molecular Magnetism*. VCH Publishers, New York
47. Baker GA, Rushbrooke GS, Gilbert HE (1964) High-temperature series expansions for the spin-1/2 Heisenberg model by the method of irreducible representations of the symmetric group. *Phys Rev* 135:1272–1277
48. Shi XX, Chen QJ, Chen XL, Zhang Y, Kurmooc M, Zeng MH (2019) Monitoring fragmentation and oligomerization of a di- μ -methoxy bridged copper(II) complex: structure, mass spectrometry, magnetism and DFT studies. *Dalton Trans* 48:13094–13100
49. Escuer A, Vicente R, Mernari B, Gueddi AE, Pierrot M (1997) Syntheses, structure, and magnetic behavior of two new nickel(II) and cobalt(II) dinuclear complexes with 1,4-dicarboxylatopyridazine. MO calculations of the superexchange pathway through the pyridazine bridge. *Inorg Chem* 36:2511–2516

Publisher's Note Springer Nature remains neutral with regard to jurisdictional claims in published maps and institutional affiliations.